Natural Hazards
https://doi.org/10.1007/s11069-024-06466-8

ORIGINAL PAPER

Compounding effects of changing sea level and rainfall regimes on pluvial flooding in New York City

Mahshid Ghanbari[1] · Tyler Dell[2] · Firas Saleh[3] · Ziyu Chen[4] · Jennifer Cherrier[5,6] · Brian Colle[7] · Joshua Hacker[8] · Luke Madaus[8] · Philip Orton[4] · Mazdak Arabi[1]

Received: 3 February 2023 / Accepted: 29 January 2024

Abstract
Coastal urban areas like New York City (NYC) are more vulnerable to urban pluvial flooding particularly because the rapid runoff from extreme rainfall events can be further compounded by the co-occurrence of high sea-level conditions either from tide or storm surge leading to compound flooding events. Present-day urban pluvial flooding is a significant challenge for NYC and this challenge is expected to become more severe with the greater frequency and intensity of storms and sea-level rise (SLR) in the future. In this study, we advance NYC's assessment of present and future exposure to urban pluvial flooding through simulating various storm scenarios using a citywide hydrologic and hydraulic model. This is the first citywide analysis using NYC's drainage models focusing on rainfall-induced flooding. We showed that the city's stormwater system is highly vulnerable to high-intensity short-duration "cloudburst" events, with the extent and volume of flooding being the largest during these events. We further showed that rainfall events coupled with higher sea-level conditions, either from SLR or storm surge, could significantly increase the volume and extent of flooding in the city. We also assessed flood exposure in terms of the number of buildings and length of roads exposed to flooding as well as the number of the affected population. This study informs NYC's residents of their current and future flood risk and enables the development of tailored solutions to manage increasing flood risk in the city.

Keywords Pluvial flooding · Sea-level rise · Climate change · Hydrologic and hydraulic model

1 Introduction

Urban flooding from extreme rainfall (i.e., urban pluvial flooding) poses public safety risks and threats to human life and property across the world (Jha et al. 2012). In New York City (NYC), which has approximately 70% impervious cover and extensive combined sewers, urban pluvial flooding is a well-known problem (NYC Stormwater Resiliency Plan 2021). Extreme rainfall can also be compounded with the co-occurrence of high sea levels either from tides or storm surge events and cause compound flooding events (Orton et al. 2012;

Extended author information available on the last page of the article

Bevacqua et al. 2019), like that caused by Tropical Storm Irene in 2011(Wahl et al. 2015). Urban pluvial flooding in NYC is not a present problem of concern but is likely to intensify in the future due to the increasing frequency and magnitude of extreme rainfall events, sea-level rise (SLR), and increasing frequency and magnitude of surge events and tides (Lenderink and Van Meijgaard 2010; Sillmann et al. 2013; Walsh et al. 2014; NPCC 2015; Ghanbari et al. 2019).

Several hurricanes, storms, tropical, and subtropical cyclones affected NYC during recent decades with either heavy rainfall and cloudburst, storm surge, or compound flooding. The remnants of Hurricane Ida (September 2021) resulted in ~ 7 inches of rain across parts of NYC, including a record rate of ~ 3 inch hr^{-1} at Central Park (Wolfe et al. 2021). The NYC sewer system is only designed for 0.6–1.5 inch hr^{-1} rates, so widespread flooding occurred, and 13 people lost their lives, mainly in basement apartments in Queens. Remnants of Hurricane Elsa (July 2021) caused up to 2.3 inches of rainfall that triggered flooding in many parts of the city (New York Times 2021). In August 2020 Tropical Storm Isaias brought 3 to 6 inches of rain with wind gusts of 50 to 80 mph. Hurricane Sandy (October 2012) was the largest superstorm ever recorded in the Atlantic Basin that caused an estimated $60 billion in damages, mostly from coastal flooding (Diakakis et al. 2015). Hurricane Irene (August 2011) with landfalls of up to 60 mph wind was a destructive hurricane affecting most of the East Coast of the U.S. with estimated total damage of almost $15.6 billion (Avila and Cangialosi 2011; Fieser 2011). Hurricane Floyd (September 1999) with wind gusts of up to 150 mph produced rainfall up to 13 inches from North Carolina to northern New Jersey and caused monetary damage estimated at $6.5 billion. Collectively these recent events—as well as historical trends—demonstrate that it is only a matter of time before NYC is hit with another, and perhaps more severe rainfall flooding event. Pressures on the city's aging combined sewer systems are on the rise due to the increased frequency and intensity of storms, SLR, and land-use change (Yohe and Leichenko 2010; Karamouz et al. 2015).

The NYC Panel on Climate Change (NPCC 2015) anticipates that by the end of the century, annual rainfall could increase as much as 25% and the number of days with more than one inch of rainfall could increase 1.5 times in NYC. A study by Depietri and McPhearson (2018) reveals that the number of days with more than 1.75 inches of rainfall (extreme rainfall) has increased over the past 140 years in NYC. Also, New York has seen an increase of 2.5 inches in summertime rainfall in the past 60 years alone (Cappucci 2019). Climate projections reveal that this increasing trend will continue, and NYC will likely experience significantly increased rainfall in the future (NYDEC 2019; NYSDEC 2021). Furthermore, SLR (Rahmstorf 2007; Sweet et al. 2017; Ghanbari et al. 2019, 2021) and increasing frequency and magnitude of surge events and tides (Rahmstorf and Coumou 2011; Hallegatte et al. 2013; Bevacqua et al. 2019; Ganguli et al. 2020) are also increasing the risk of urban pluvial flooding by submerging outlets and decreasing the capacity of storm sewer systems. High tides and surges made higher by SLR temporarily limit the ability of stormwater infrastructure to drain streets as designed and prolong flooding events.

Considering the increased risk of flooding, the complex network of natural and built stormwater conveyance systems in NYC is increasingly overwhelmed, leading to flooding and water quality degradation. Without adopting appropriate strategies that prepare NYC for the impacts of future extreme flood events, damages to public and private property will increase (Wolfe et al. 2021). While NYC has made significant strides in stormwater management and resilience, challenges persist in evaluating future storm events and flood occurrence data. The ongoing nature of stormwater mitigation projects and studies highlight a concerted effort to address the challenges posed by pluvial flooding and compound

flooding in NYC. The success of these projects is contingent on access to accurate data, robust modeling tools, and a deep understanding of the complex dynamics involved in stormwater management. As such, addressing the aforementioned gaps in storm events and flood occurrence data is paramount to ensuring the effectiveness of these mitigation efforts. For NYC to develop and accomplish initiatives to improve service reliability and resiliency of stormwater systems, it is important to identify and consolidate knowledge of current and future stormwater issues. Achieving this goal requires consideration of multiple urban pluvial flood drivers including understanding of localized sewer network capacity and overland drainage pathways, development of current and future rainfall hyetographs, and consideration of tidal conditions and climate change.

The vulnerability of NYC to coastal flooding is well known after Sandy (Colle et al. 2015; Orton et al. 2016), but less is known about the compound risk of surge, SLR, and rainfall, since there have been no coupled modeling efforts to characterize them. To understand complex and evolving urban pluvial flood drivers as well as evaluate flood hazards and exposure in NYC under different storm events and sea-level conditions, we developed a citywide Hydrologic and Hydraulic (H&H) model to simulate various storm scenarios under current and future climatic conditions. This is the first citywide analysis using NYC's drainage models focusing on rainfall-induced flooding. Several analyses have been conducted in the city in the past, but they were localized and mainly driven by coastal flooding rather than inland rainfall. Using the developed H&H model we simulated urban flooding based on the combined impact of rainfall and coincident tidal/surge conditions applied to sewer outfalls.

This study advanced NYC's assessment of present and future exposure to urban pluvial flooding. Specifically, the objectives were to (1) investigate how variation in storm intensity and duration affect the volume and extent of citywide flooding using a citywide H&H model, (2) assess the citywide exposure to flooding in terms of inundated roads and buildings for each simulated storm scenario, (3) evaluate the exacerbating effects of extreme rainfall compound with SLR or storm surge on urban flood events, and (4) characterize the exposure of affected population under different storm scenarios and sea-level conditions. The results of this study provide valuable insights into the potential impact of rainfall intensity and duration, as well as the compounding effect of SLR or storm surge, on urban pluvial flooding in NYC and can serve as a basis for developing effective strategies and policies aimed at reducing flood risk and mitigating its associated impacts on the city's residents and infrastructure.

2 Materials and methods

2.1 Study area

The NYC stormwater system is comprised of an extensive network of over 7,400 miles of sewer pipes that collect sanitary sewage and stormwater, and 14 Wastewater Resource Recovery Facilities (WRRFs)[1] (Fig. S1, Supplementary Information). Approximately 60% of NYC's sewer system is used to convey both sanitary and storm flows (combined sewer

[1] 26th Ward, Bowery Bay, Coney Island, Hunts Point, Jamaica, Newtown Creek, North River, Oakwood Beach, Owls Head, Port Richmond, Red Hook, Rockaway, Tallmans Island, and Wards Island.

system). For the remaining, separate storm and sanitary sewers direct runoff and sewage to waterbodies and WRRFs, respectively (NYC DEP 2021).

2.2 Storm scenarios

NYC experiences a diverse range of storm types, each with unique characteristics. These storms have the potential to trigger extreme rainfall events, resulting in urban pluvial flooding, or, in some cases storm surge that may lead to compound ("Multivariate"), spatially, or temporally compounded flooding (Zscheischler et al. 2020). Convective storms primarily occur during the warm season, exhibiting temporal scales spanning from minutes-to-hours and spatial scales capable of encompassing entire regions of NYC (Lombardo and Colle 2010; Colle et al. 2012), often accompanied by rainfall rate that can exceed 2 inch hr^{-1} (Smith and Rodriguez 2017). During the late summer and fall, tropical cyclones, associated with low-pressure systems, can move northward along the east coast and cause an extensive region of heavy rainfall over a 12- to 24-h period that extends hundreds of miles ahead of the storm (Atallah and Bosart 2003) and often brings storm surges, contributing to compound flooding. Similarly, cool-season extratropical storms can produce extensive regions of heavy rainfall, often lasting several hours, and could also coincide with storm surges may lead to compound flooding. Considering the diversity of storm types in NYC, conducting a comprehensive flood risk assessment necessitates the incorporation of scenarios that encompass a broad spectrum of factors, including rainfall intensity and duration, tidal levels, storm surges, and the impact of climate change.

To this end, after several iterations of consultation with NYC agency stakeholders, twelve storm scenarios were created for this study. These scenarios cover a range of NYC rain and coastal sea-level parameters and also address specific city needs for emergency management, planning, and design. The storm scenarios included preexisting NYC design storms, historical storms of special interest, and simulated storms with intensities that match observed rainfall statistics to capture specific rainfall intensity, frequency, and duration. Focusing on assessing the potential multivariate simultaneous compounding for all storm scenarios, we modeled offshore tide and, when indicated, storm surge and SLR data were matched and applied as boundary conditions. Eight main storm scenarios included only time-varying tides without the compounding effect of surge or SLR. Four storm scenarios were repeated a second time to evaluate the compounding effect of surge or SLR. The description of storm scenarios and the methods used to create them are provided in the following sections, and the final scenarios are summarized in Table 1. The remainder of this section details the methods to construct input for the H&H modeling of each scenario.

The storm scenarios covered a wide range of intensity with return periods from 1-year up to an approximately 10,000-year event, and intensities ranging from 0.3 to 4.3 inches hr^{-1}. The latter was the worst historical rain event known to have occurred in the region at the time of this study (Scenario 6, SC6). This event, a very localized storm that affected Islip, NY (~ 70 km east of NYC) in August 2014, had 12.9 inches of rain over 3 h. Hurricane Ida (August 2021) which occurred after this study is similar to this Islip event, also with 3–4 inches hr^{-1} rates. Rain durations in modeled scenarios varied from 1- to 24-h events, with intensity varying and peaking over periods as short as 5 min, capturing the range of rain characteristics from common convective downpours to hurricane events. The storm set included specific cases for the Department of Environmental Protection (DEP) drainage standard (SC5), two for the Office of Resilience and Recovery (ORR) Climate Resiliency Design Guidelines (CRDG) (SC7, 8), as well as one for Emergency

Table 1 Characteristics of the storm scenarios (SC represents scenario, Future return period refers to the return period in 2050s)

Storm scenario	Intensity (in/hr)	Depth (in)	Duration (hours)	Current return period (years)	Future return period (years)	SLR (feet)	Surge (feet)
SC1	1	1	1	< 1	< 1	–	–
SC1 + SLR	1	1	1	< 1		2.3	–
SC2	1.22	1.22	1	1	< 1 < 1	–	–
SC3	1.77	1.77	1	5	< 5	–	–
SC3 + Surge	1.77	1.77	1	5	< 5	–	1.3
SC4	3.66	3.66	1	100	Between 50–100	–	–
SC5	0.85	2.55	3	5	< 5	–	–
SC6	4.29	12.86	3	~ 1000	n/a	–	–
SC7	0.18	4.32	24	5	< 5	–	–
SC7 + surge	0.18	4.32	24	5	< 5	–	2.9
SC8	0.3	7.2	24	50	> 5	–	–
SC8 + surge	0.3	7.2	24	50	> 5	–	3.1

Management's Flash Flood Hazard Plan (SC1). Through these storm scenarios, we were able to investigate the effect of storm events of varying intensity and duration, SLR, and surges on flood characteristics and exposure in NYC.

The following sections provide a detailed explanation of the development of storm scenarios. It begins by explaining the univariate and bivariate extreme value analysis, followed by an exploration of offshore sea-level forcing for tide and storm surge. The sections then progress to an explanation of future sea-level rise scenarios, accompanied by methods for estimating the effects of climate change on rain intensities.

2.2.1 Univariate extreme value analysis

Hourly observed rainfall data from 11 rain gauges within 15.5 miles of Central Park, plus 5 others on Long Island, were used in a frequency analysis that provided eight main storm scenarios. The inclusion of the Long Island rain gauges within the NYC rain dataset led to more conservative rainfall depths for storm scenarios by increasing depth and variability in the dataset for high-return period storms. Rain-gauge years of operation varied, but the entire 16 rain-gauge datasets covered a whole period of record from 1948 to 2013. All station-years of data were pooled together to total over 700 station-years of data representing the "coastal plain" rain hazard. This approach adopted the assumption that the low-lying areas all have very similar rain intensity-duration probabilities, and reduced uncertainty in longer return periods (e.g., 100-year). A sliding time window was used to sum the rain total depth for a specific duration of time by moving hour by hour over the entire rain record.

Extreme value analysis using generalized Pareto distribution (GPD) was performed separately for 1-, 3-, and 24-h rain durations (Li et al. 2014) and applied to peaks over a threshold chosen to have approximately one event per year. For each duration, the peak rain totals were identified throughout the record. Peak rain totals were the maximum rain totals for the duration, with no overlapping events allowed. Empirical return period points estimated using the Gringorten plotting position formula were used to graphically evaluate the reasonableness of GPD in capturing the tail of the distribution. While formal goodness-of-fit tests would have been a stronger approach, visual examination was a useful form of quality control in a very short-term city-funded project under time pressures. The sample results are shown in Fig. S2 in Supplementary Information. Rain totals for each return period and duration were used to create intensity–duration–frequency (IDF) curves. IDF curves represent the probability of rainfall occurrence by using return periods to specify the intensity of rainfall for a given duration and are usually used to design sewers for runoff conveyance in NYC. Intensity was defined by the rain total divided by the duration, and frequency was defined by the return period. Methods for estimating climate change effects on rain intensities are presented in Sect. 2.2.5.

2.2.2 Bivariate extreme value analysis for extreme rainfall/storm surge compound scenarios

The joint probability of extreme rainfall and storm surge was estimated to create the scenarios of compound flooding. Since this study primarily focused on urban pluvial flooding, the analysis only considered compound events conditioned on the occurrence of extreme rainfall, as opposed to compound events conditioned on the occurrence of storm surge events. The joint occurrence of rain and surge was evaluated using rank correlation and linear regressions of different percentiles of surge as a function of rainfall.

For the bivariate analysis, we employed slightly different rain-gauge datasets, in that hourly rain data from all rain gauges in a radius of 15.5 miles around the Battery tide gauge site (14 total) were used. These gauge data were then averaged to estimate a spatial average. This focused the analysis on regional rain events, as opposed to localized convective rain events, as the former is much more likely to be accompanied by storm surge events (Wahl et al. 2015). Hourly storm surge data were used for the period of record overlapping the rain data from the Battery tide gauge. The storm surge value was obtained by subtracting astronomical tide data created using harmonic analysis from the total water level (Pawlowicz et al. 2002). Unlike previous studies that used maximum surge within a window of ± 1 day of extreme rainfall event (Wahl et al. 2015), we used the maximum surge during the rainfall event, since the relatively small NYC sewersheds have very short times of concentration (e.g., minutes-to-hours). The significance of statistical dependence between the paired data was assessed using Kendall's rank correlation coefficient and significance is assessed using $\alpha = 0.05$.

For the percentiles approach, a 20-sample sliding window was used to compute a percentile of surge running from the highest rain to the 80th highest rain. The generalized extreme value (GEV) distribution curve was used to fit the storm surge maxima in order to estimate the 50th, 75th, and 90th percentiles surge in each 20-sample window, then a linear model was fitted to each of these percentiles. To provide for high-end, risk-averse planning with the storm scenarios, the linearly modeled 90th percentile surge was chosen as the compound surge for extreme rain events. As a preference requested by NYC stakeholders, prior climate risk projections have also used 90th percentiles for conservative, risk-averse planning (e.g., Gornitz et al. 2019). The linear modeling of each surge percentile as a function of rainfall was chosen as a simple method of interpolating (or slightly extrapolating) from the historically based percentiles. However, because the modeled values are within the range of historical events, using nearest-neighbor empirical observed values would give a similar result.

2.2.3 Offshore sea-level forcing for tide and storm surge

Tides have twice-daily excursions of 2–3 ft above and below mean sea level around NYC (Orton et al. 2012) and are an important additional source of compound flooding. Rainfall occurs with random timing relative to tides. All storm scenarios in this study are essentially forms of compound events, either including only rainfall and tide, or including rainfall, tide, and storm surge. The coupling of rainfall and these offshore water levels occurred through provision of time series of hourly offshore water level as open boundary conditions (OBCs) for the H&H model. Spatially and temporally varying water-level data, from preexisting regional hydrodynamic model simulations, were utilized for these OBCs. The use of the model results, from the New York Harbor Observing and Prediction System (NYHOPS), captured the spatial variation in tides around the city (Long Island Sound and Jamaica Bay have much larger tide ranges than Manhattan; Orton et al. 2016), as well as a small nonlinear enhancement of tide range by SLR in Long Island Sound (Kemp et al. 2017).

The twelve modeled storm scenarios were coupled with tide data as OBCs, such that the 1-h duration events had high tide within the hour of maximum rain intensity and the 24-h duration events had multiple high and low tides within the simulation. Compound storm surge simulations included a constant storm surge value on top of the temporally and spatially varying tide. For the 1-h and 3-h events, the high tide peaked at the center of the

rain period at all locations across the city. The goal here was to account for possible high-tide effects on flooding near the coast (e.g., how tide blocks sewer outfalls). Again, some of these choices represent conservative approaches, generally the preference of the NYC stakeholders when we are faced with the limitations of the project in the number of simulations and computational expense.

2.2.4 Future sea level

For future scenarios, sea-level rise was determined based on high-end (90th percentile) projections of the 2050s, as reported by the NYC Panel on Climate Change, NPCC (Horton et al. 2015). The sea-level rise projections for NYC are based on 24 Global Climate Models (GCMs) and two representative concentration pathways, RCP 4.5 and 8.5. The projections include the low estimate (10th percentile), middle range (25–75th percentile), and high estimate (90th percentile). For the future climate at the 2050s, a sea-level rise projection of 30 inches above a baseline at 2000–2004 was applied. With this projection, the 2050s sea level was projected to be 29.1 inches NAVD88. This sea level was simply superimposed upon the offshore boundary condition water levels of tide or tide and surge. It should be noted that the "present-day" simulations incorporate the year 2018 mean sea level, which is 1.7 inches NAVD88 (Chen et al. 2017).

2.2.5 Present-day and future hyetographs

The extreme value analysis provided intensities for durations selected in the analysis, and the associated frequencies. Hyetographs for those intensities and durations, both present day and in the future, were based on simulated storms that match the present-day and projected future conditions. Similar to the surge and sea level, the 90th percentile of rainfall intensities were selected.

Overall, climate projections for rainfall remain quantitatively uncertain since several factors may contribute to future changes in rainfall. These factors include a change in the types of events that produce rainfall in a given area, as well as a change in the frequency, duration, and intensity of events. Future intensities for extreme-event hyetographs were derived primarily by adapting the intensity changes projected by Castellano and DeGaetano (2017). Those were based on Representative Concentration Pathway (RCP) 8.5, and approximately the year 2050. The effects of climate change reported in that work were applied to the IDF curves derived in this work. Castellano and DeGaetano (2017) did not evaluate or scale frequencies below 5-year return periods. Intensities for common events, expected more frequently than a 5-year return period, were climate scaled with a quantile-matching approach. The 1 inch in an hour event was also scaled via quantile matching.

Model output from a dynamical downscaling experiment (Rasmussen and Liu 2017) provided the information needed for scaling via quantile matching. That experiment consisted of a historical (2000–2013) period simulation at 4-km grid spacing covering the Continental US, and a counterpart end-of-century simulation produced by adding a large-scale change to the boundary conditions of the downscaling model to simulate the end-of-century climate. That change was a multi-model mean between the historical period climatology and the 2071–2100 period, computed from many CMIP5 GCMs. The interested reader should refer to Liu et al. (2017) for further experiment details. For these purposes, it is sufficient that the simulations were high resolution and that the experiment can provide scaling for intensity and duration, but not frequency. Samples of rainfall intensities for the

historical period and future period were assembled for the region around NYC. Assuming linear changes in quantile intensities, intensity change from early century to late century was interpolated, for each quantile, to 2050. As an example, the quantile associated with 1 inch in 24 h intensity increases by approximately 22% from early to mid-century.

Realistic temporal structure of hyetographs at 1, 3, and 24-h durations for current and future climates was given by hourly output from dynamical simulations. A catalog of 635 historical simulations was developed, based on a conservative threshold of 0.4 inch in 24 h observed by Global Historical Climate Network (https://www.ncdc.noaa.gov/ghcn-daily-description) stations within NYC (LaGuardia, John F. Kennedy International Airport, and Central Park) during the period 1979–2016. Events exceeding that threshold were simulations with the Weather Research and Forecasting (WRF) version 3.9.1 (Skamarock and Klemp 2008). Consecutive days exceeding 0.4 inch in 24 h were aggregated into individual events of 1–7 days, and events under 1.2 inches in total were discarded. This approach allows for both short and longer duration events that can cause flooding. For a given intensity and duration, the time series at WRF grid points over land and within 60 miles of the Battery, and within every simulation, was searched to find the closest match in accumulated precipitation during the duration of interest. That time series served as the hyetograph for each H&H simulation.

2.3 Hydrologic and hydraulic model

A set of H&H models were developed to cover all 14 sewersheds across the city, each coupled 1-dimensional (1-D) stormwater components with two-dimensional (2-D) overland flow (Fig. 1). The twelve storm scenarios were simulated with the citywide H&H model to examine flood characteristics and exposure under varying rainfall events and sea-level conditions. The H&H models simulated stormwater flooding scenarios from rainfall and compound (rainfall and storm surge) events to better understand vulnerability to different types of flooding. In the following, the approach and methodology for developing and validating the models are described.

2.3.1 InfoWorks models

We used the InfoWorks Integrated Catchment Model (ICM) V.9.0 to facilitate integration with the NYC Department of Environmental Protection's (NYC DEP's) existing sewer models. InfoWorks conceptualizes the system as a series of processes between several major components, including (1) an atmospheric component, (2) a land surface component, and (3) a routing component (Fig. 1). The atmospheric component was represented by a time series of rainfall inputs to the system. The land surface component was represented by a 2-D computational mesh, which received rainfall from the atmospheric component in the form of rainfall time series. It then conveyed simulated surface runoff to the routing component, which contained a network of conveyance elements modeled with manholes (known as nodes) and pipes (known as link objects) to route runoff to wastewater resource recovery facilities and outfalls (or terminal nodes) of sewersheds. The drainage of the outfalls was determined by the water levels (storm surge, tides) for each storm scenario. Inflows to the routing component came from surface runoff and external outflow from contributing drainage areas. The model accounted for full dynamic wave flow routing (Rossman 2015), which allowed for the simulation

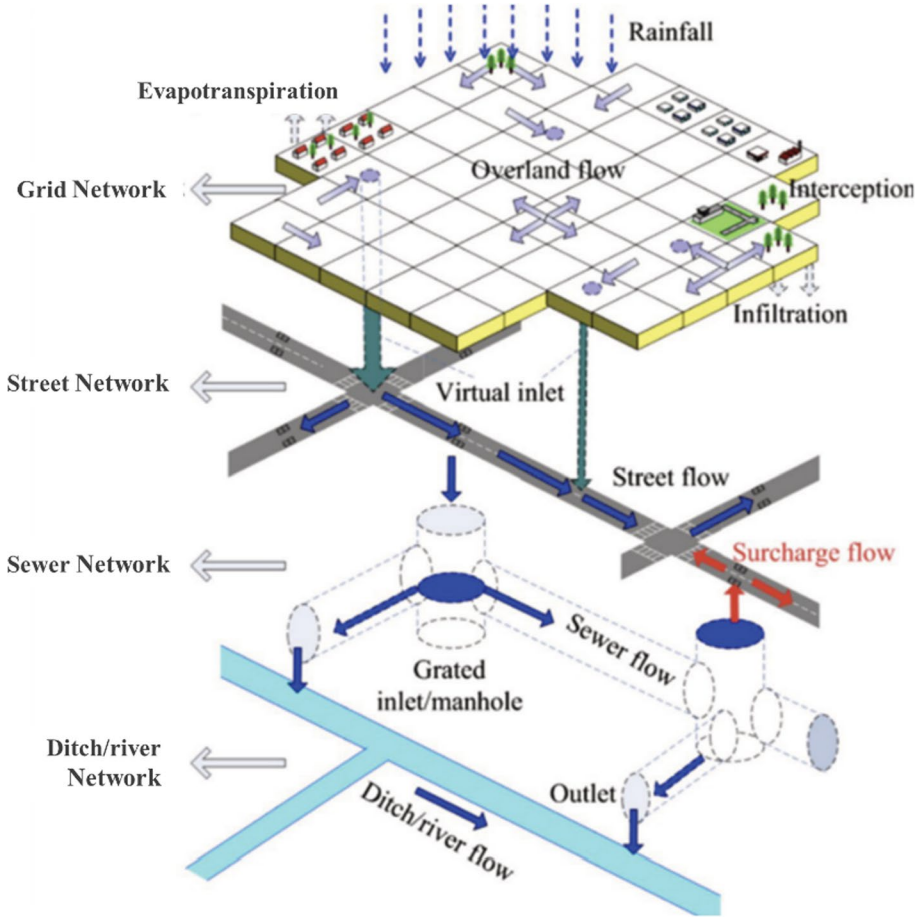

Fig. 1 Schematic of simulated processes in coupled stormwater system and overland flow

of complex hydraulic interactions such as backflow effects and pressurized flow in the pipes and flow exchange between the streets and the sewer system.

We migrated the existing InfoWorks Catchment System (CS) models to InfoWorks ICM to simulate the connectivity between the stormwater system and the surface. This connectivity required manipulating objects within InfoWorks ICM to handle these surface–subsurface interactions. The main conceptual difference between the original NYC DEP models and the updated surface–subsurface model was how the model simulated rainfall data and overland flooding. The updated models simulated rain directly onto the 2-D computational mesh instead of defined sub-catchments. The previous InfoWorks CS models could not simulate overland routing and flooding, but the two-dimensional component of InfoWorks ICM simulated the flow path of water by applying St. Venant's equation to each computational cell in conjunction with the DEM. Lastly, the updated models also recognized different sources of inflow into a given cell; thus, InfoWorks ICM no longer stored overflow from manholes but treated it as an additional influx of water into a given cell.

To develop the model, stormwater conveyance components were extracted from the existing DEP InfoWorks 1D sewer models. Data on the stormwater systems on private property, infrastructure areas not owned and operated by NYC DEP, and manholes not included in InfoWorks 1-D models were not available for inclusion in the model. Geographic Information System (GIS) preprocessing algorithms were used to enable representation of spatial data in InfoWorks ICM. The most recent 1-foot resolution, bare-earth digital elevation model (DEM) was used (NYS 2018) to represent the terrain and create the 2-D model within InfoWorks ICM, which uses a triangular unstructured surface mesh. The variable mesh resolution in ICM provides the ability to decrease the triangle size in areas of complex geometries or greater interest to provide higher resolution results.

Pervious surfaces were represented in InfoWorks ICM via roughness and infiltration polygon(s), which were both derived from the NYC Parks Department's land-use data. Pervious surfaces were extracted from the land-use data and considered to infiltrate rainfall into soils based on the Horton equation (Horton 1941). The basic premise of the Horton equation is that the amount of infiltration within the soils is based on the hydrologic soil group classification. The parameters for the Horton equation were selected to provide the best validation, and applied uniformly across the computational meshes. We applied the "moderate" infiltration parameters in InfoWorks ICM, which are 200 mm h^{-1}, 12.7 mm h^{-1}, and 2 h^{-1} for the initial infiltration rate, the final (limiting) infiltration rate, and soil-specific decay constant, respectively.

2.3.2 Model validation

Validation of the citywide H&H model was carried out based on model performance checks and quantitative comparison of areas of flooding predicted by the model against historic flooding records. First, we compared the modeled total inflow to each wastewater resource recovery facility (WRRF) with observed inflow during a historic rainfall event on August 14, 2011. This storm had approximately two months' worth of rain in a single day. Second, we compared flood extents predicted by the model for specific storms with 311 complaints of street flooding. 311 is a platform in NYC where people can file issue reports to the city administration or the government. The lack of spatially distributed observations of flood depth in the study domain necessitated the use of 311 calls as a proxy for flooding. The results provided confidence that the simulations are accurately representing the primary areas subject to flooding, though these data were not sufficient to validate the depth of flooding. Comparison of the flood extents to 311 complaints was performed by selecting complaints that had observed rainfall magnitudes similar to specific rainfall scenarios, namely a 1-inch,1-h storm (SC1), and a 2.55-inch, 3-h storm (SC5).

In the first validation, simulated flow volumes and peak flow rates were compared with observations at each of the City's WRRFs, which represent the most downstream portion of the conveyance system. According to the NYC Citywide Watershed Model Recalibration guidance document (Infoworks 2012), the difference between observed and modeled peak flow rates at each significant peak should be in the range of + 25% to − 15%, and the differences between observed and modeled flow volumes between + 20% to − 10%. The difference between the simulated and observed peak flow rates across the sewersheds all fell within the preferred range except in one instance (Fig. S4, Supplementary Information). With respect to volumes, there were six instances where the difference between the simulated and observed volumes fell outside the preferred range of + 20% to − 10% (Fig. S5, Supplementary Information). However, the results were within expected uncertainties; the

relative volume variability at the WRRFs was largely the same in the observations and simulations (Table S1 and S2, Supplementary Information).

We filtered 311 complaints for the root cause of "street flooding" between 2014 and 2018 and then confirmed that each of these complaints corresponded to a date in which there was recorded rainfall at John F. Kennedy (JFK) airport. A correlation indicator was then applied to depict the percentage of cells with a maximum flood depth threshold exceeding 0.25 ft, to eliminate potential false positives obtained within a 100-ft buffer area around these 311 complaints. The correlation indicator was calculated for the selected events across NYC using the 311 complaints between 2014 and 2018 as the number of points with maximum underlying depth greater than 0.25 ft divided by the total number of 311 points (Saleh et al. 2017). A total of 10,067 311 complaints for street flooding were identified (Fig. S6, Supplementary Information). We then identified specific events that corresponded to the rainfall accumulation and duration for two of the modeled storm scenarios; the 1-inch, 1-h storm (SC1) and the 2.6-inch, 3-h (SC5). Given the uncertainty in the 311-call data itself, the correlation between 311 complaints and modeled flooding across these three events was high (Table S3, Supplementary Information).

2.4 Exposure data

The NYC Department of City Planning annually produces the Primary Land Use Tax Lot Output (PLUTO) file, which contains information about each tax lot in the city, including the building class, land-use type, and other variables about the structure and location. Building and land-use Information were obtained from MapPluto 2019 (https://www1.nyc.gov/site/planning/data-maps/open-data/dwn-pluto-mappluto.page). The buildings were then classified into three main categories based on their land use: residential (R), industrial (I), and commercial (C). A detailed breakdown of building classes in each land-use category can be found in Table S4 of the Supplementary Information.

3 Results

3.1 Univariate extreme value analysis (EVA) results

A comparison of our final rain EVA estimates with NOAA Atlas 14 at Central Park (NOAA 2014) shows the similarity between estimates for 1- and 5-year return periods (Fig. 2). For 50- and 100-year return periods, our estimates have a higher value of intensity than do the NOAA Atlas 14 for durations under 3 h. The difference is likely due to the pooling of rain gauges, including Long Island (where the Islip event occurred with the most extreme 1–4 h rainfall intensities in the region), while NOAA Atlas 14 used rain data from only one rain gauge at Central Park. This is the reason to use the regional analysis including Long Island, for conservative planning.

Figure 3, the left panel, shows a fuller picture of EVA results, in which the entire range of possible rain depths is depicted from 1 to 48-h duration and 1-to-1000-year return period. All the storm scenarios are based on the rain totals shown here. For each extreme rain value, there is a corresponding 95% confidence interval (Table S5, Supplementary Information), estimated by bootstrapping, used both to convey uncertainty and to assist in matching with WRF simulation results. The original data were resampled 1000 times, and a GPD curve was fitted for each new dataset. Next, the 97.5th and 2.5th

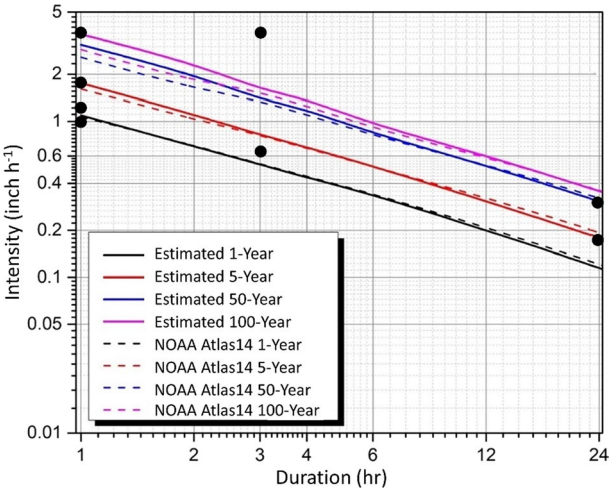

Fig. 2 Present-day rain IDF curves compared between our estimates and NOAA Atlas 14. Storm scenarios are plotted as points

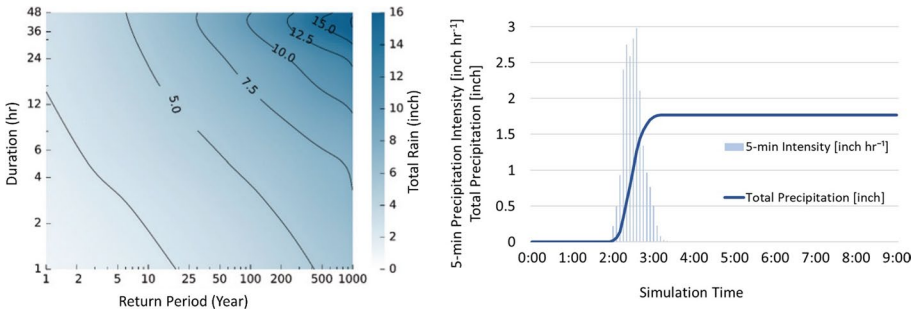

Fig. 3 (Left panel) Rainfall total depth estimates (inches) for various return periods and durations. (Right panel) Hyetograph for storms scenario 3 (1.77-inch, 1-h)

percentiles were chosen to represent the 95% confidence interval for each return period. Bootstrap uncertainty analysis was performed on both individual rain gauges and pooled datasets. Several additional sensitivity analyses were performed to test the rationality and stability of the final results, including adding one more station to the pooled dataset, using gauges within different radii of NYC other than 15.5 miles (e.g., 31 miles), and comparing EVA results from different individual rain gauges. The uncertainty was impacted by several aspects of the chosen methods. Uncertainty increased by the inclusion of the diverse rain data from the entire coastal plain rain-gauge sample, including 6 rain gauges from Long Island. Uncertainty decreased by pooling the data to increase the sample size. As is typical, there is substantial uncertainty, represented by a large confidence interval, for high-return periods (e.g., greater than 200 years).

Modeled rainfall time series for all the storm scenarios are presented as plots in the supplementary information (Fig. S7-S14), and an example (SC3) is presented in Fig. 3, right panel. These 5-min resolution results were then applied to the H&H modeling to create final storm scenario simulations.

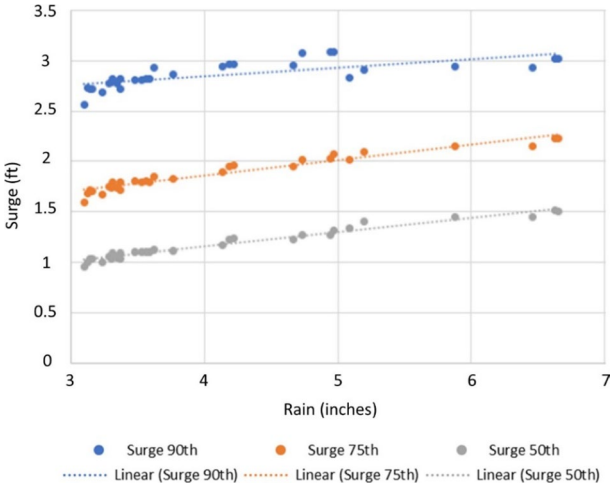

Fig. 4 Relationship between the 90th, 75th, and 50th percentile compound surges and 24-h total rain totals

3.2 Bivariate analysis of rain/surge compound flooding

Rain and surge for 24-h storm duration have a Kendall rank correlation coefficient of 0.23 which is significant with p-values of around 0.01. Rain and surge for the 1-h storm duration have low Kendall rank correlation coefficients, which are not significant at the 0.05 level with p-values around 0.10. The result that 24-h rain correlates with surge, whereas 1-h rain does not, likely arises because synoptic weather systems that cause high 24-h rainfall events are large-scale and cause storm surge, whereas convective rain systems that cause high 1-h rain are small scale and do not. Nevertheless, completely ignoring any correlations risks underestimating the compound flood hazard (Moftakhari et al. 2017).

The results for the percentiles approach to defining the joint occurrence of extreme rain and surge are shown in Fig. 4 (24-h rain) and S15 (1-h rain). A positive linear trend between various percentiles of compound surge and 24-h rain total depths is evident, whereas no trend is evident with surge with 1-h rain intensity, both consistent with the rank correlation analysis. The fitted linear equations (90th percentile) were used to estimate the compound surges for specific 1-h and 24-h rain total depths. Thus, 2.9 and 3.1 ft surge was utilized with the 24-h rain events SC7 (5-year, 4.31 inches) and SC8 (50-year, 7.2 inches), respectively, and 1.3 ft surge was utilized for the 1-h rain event SC3 (5-year, 45-mm).

3.3 Flood characteristics and exposure

The overland model outputs were provided as maximum flood depth above ground for all the storm scenarios. The maximum values associated with maximum flood depth values were produced at 5 ft resolution and processed into flood depth and extent maps. The final maps were developed based on the identification of areas of major (defined as 1 ft flood depth above ground and more) and nuisance flooding (defined as 4 inches to 1 ft flood depth above ground).

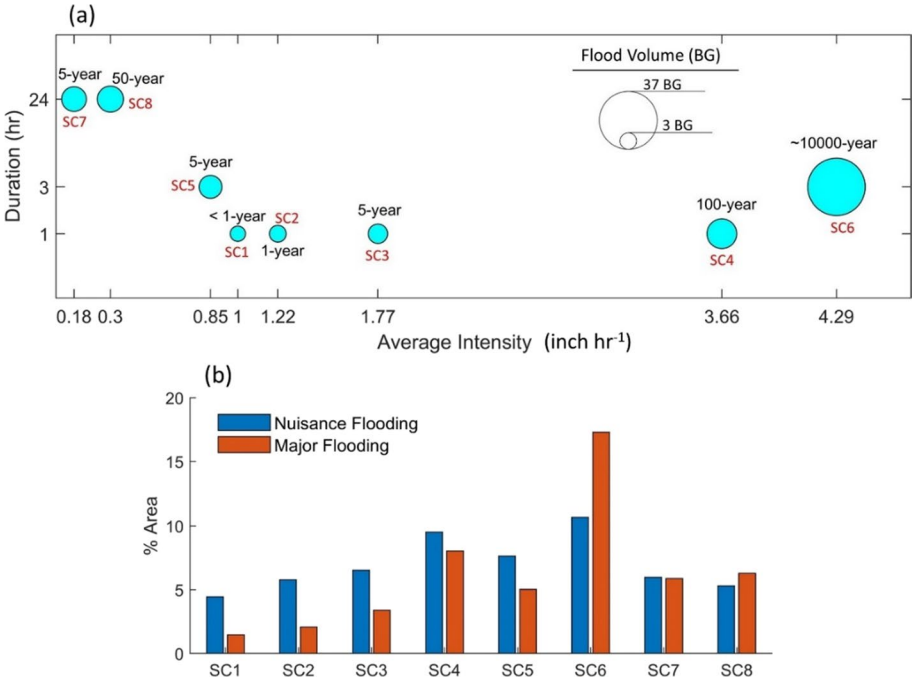

Fig. 5 Flood volume (**a**) and percentage inundation area (**b**) in NYC resulted from eight main storm scenarios. The circle size in the top panel presents flood volume in Billion Gallons (BG)

3.3.1 Flood response to storm events of varying intensities and durations

SC4 and SC6 led to the largest flood in the city in terms of both volume and extent (Fig. 5). The stormwater runoff from the high-intensity short-duration SC6, which had the highest record of average intensity (4.29 inch hr^{-1}) in the region at the time of this study, impacted ~ 28% of the city. Of this area, 17% was affected by major flooding, resulting in ~ 37 Billion Gallons (BG) of floodwater. Following that, a 100-year rainfall event with a duration of an hour and average intensity of 3.66 inch hr^{-1} (SC4) inundated 17.5% (9.5% nuisance, 8% major) area of NYC with 15 BG of floodwater. The findings illustrate how the stormwater system in NYC is stressed by high-intensity short-duration "cloudburst" events.

The standard design criterion to calculate the appropriate size of sewer pipes in NYC to be able to manage stormwater is based on a 5-year return period storm (e.g., 1.77-inch, 1-h storm). However, current design criteria are based on historical data from 1903 to 1951 and may not accurately reflect the increasing intensity and duration of 5-year return period storms due to changing climate conditions, and consequently, the NYC sewer system could fail during 5-year storm scenarios. Among three 5-year return period scenarios, the largest flood volume was caused by the 24-h storm with an intensity of 0.18 inch hr^{-1} (~ 11 BG) followed by the 3-h storm event with an average intensity of 0.85 inch hr^{-1}, and 1-h storm event with 1.77 inch hr^{-1} average intensity that led to 9 and 6 BG of floodwater, respectively. The latter storm scenario (1-h, 1.77 inch hr^{-1}) resulted in ~ 625 miles of roads being inundated by nuisance and ~ 280 miles by major flooding (Fig. 6). With a higher average

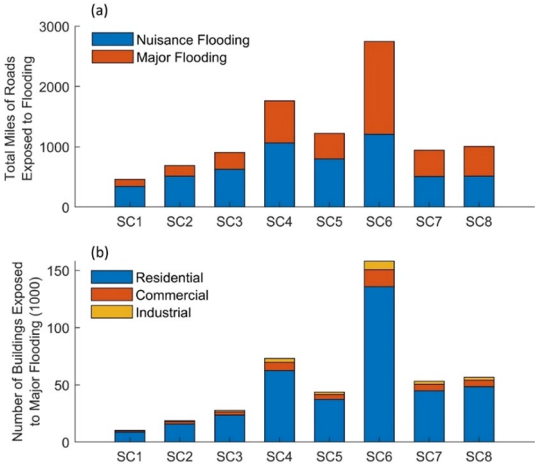

Fig. 6 **a** Total miles of roads exposed to major and nuisance flooding, **b** The number of buildings exposed to major flooding

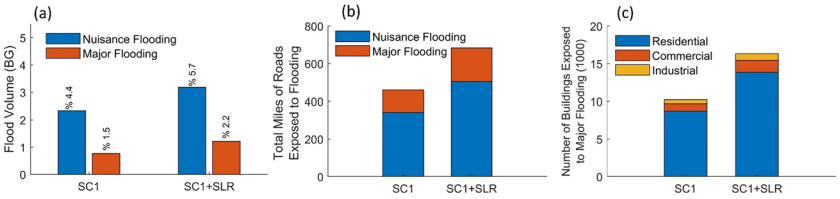

Fig. 7 Effect of 2.3ft sea-level rise on **a** flood volume and extent, **b** total miles of road exposed to nuisance and major flooding **c** number of buildings exposed to major flooding

rainfall intensity (SC3 compared to SC4) the total miles of roads exposed to nuisance and major flooding increased by a factor of ~ 1.7 (from 625 to 1060 miles) and ~ 5.9 (from 280 to 700 miles), respectively. The most extreme scenario in this study (SC6) led to ~ 1200 and ~ 1500 miles of roads being inundated with nuisance and major flooding, respectively (15% and 19% of total roads). Overall, almost one-third of NYC roads could be flooded in the case of this level of storm events.

The number of buildings in the major flooded area is depicted in Fig. 6b. It should be noted that a flooded building was defined as a building that is exposed to major flooding, as nuisance flooding events typically do not cause damage to buildings. The number of buildings affected by major flooding increased from ~ 10,000 to ~ 27,500 as the intensity of a 1-h rainfall event increased from 1 (SC1) to 1.77 (Sc3) inch hr^{-1}. As the rainfall intensity further increased to 3.66 (SC4) inch hr^{-1}, the number of exposed buildings to major flooding rose to approximately 73,000. In the case of a 3-h, 4.29 inch hr^{-1} storm event (SC6) ~ 150,000 buildings were affected.

3.3.2 Flood response to sea-level rise

SLR is one of the potential sources of expanding urban pluvial flooding in NYC (Fig. 7). It should be noted that the additional 2.3ft SLR, projected as a high-end estimate for the 2050s, does not produce permanent inundation along the waterfront in

the city, as the topography is higher than the projected amount of SLR. However, it decreases the drainage potential so that outfalls are unable to release water from the system. Figure 7 (a) reveals that more flooding (both in terms of volume and extent) could show up in the city as a result of SLR. The volume of major floodwater almost doubled with 2.3ft SLR under SC1 (1-h, 1 inch hr^{-1}). The percentage of areas flooded by nuisance and major flooding, respectively, increased from 4.4 to 5.7%, and from 1.5 to 2.2%. The increase in volume and extent of flooding due to SLR led to exposing an additional ~ 225 miles of roads to flooding (Fig. 7b) and the number of exposed buildings to major flooding elevated from ~ 10,000 to 16,000 (Fig. 7c). These findings highlight the importance of considering the potential impact of SLR in urban pluvial flood risk management and adaptation planning.

3.3.3 Flood response to compounding impacts of storm surge and heavy rainfall

We also examined three storm scenarios compounding with surge effect, namely SC3 (1.3 ft surge), SC7 (2.9 ft surge), and SC8 (3.1 ft surge). Apart from direct interactions of overland flow, storm surge at outfalls may lead to backflow into the stormwater system and upland flooding through street drains. Sediments and debris from storm surge inundation can clog pipes, storm drains, and outfalls.

The compounding effect of surge with heavy rainfall significantly exacerbated urban flooding in all scenarios (Fig. 8a). Surge of 1.3 ft compounds with a 1-h, 1.77 inch hr^{-1} storm event (SC3) increased nuisance and major flood volume by a factor of 1.5 and 2.1, respectively. Less frequent longer 24-h, 0.3 inch hr^{-1} storm events compounded with 3.1 ft surge increased nuisance and major flood volume by a factor of 1.8 and 2.4, respectively. The percentage of inundated areas with nuisance and major flooding also increased up to 1.4 and 1.9 times, respectively.

The compounding effect of 1.3 ft surge with 1-h, 1.77 inch hr^{-1} storm (SC3) did not substantially increase the exposure of roads to nuisance flooding (Fig. 8b); however, it caused a 20% increase in miles of roads exposed to major flooding (from 280 to 340 miles). 3.1 ft surge compounds with SC8 increased the milage of exposed roads to nuisance flooding from 511 to 700 miles, and major flooding from 493 to 798 miles. In other words, the milage of exposed roads became 1.5 times higher under the compound effect of 3.1 ft surge. The compound effect 1.3 ft surge with 1-h, 1.77 inch hr^{-1} storm (SC3) did not considerably increase the number of exposed buildings (Fig. 8c). The reason for this is that the compound effect 1.3 ft surge just caused some additional hotspots of flooding along the waterfront in areas subject to surge flooding and subsequently the number of affected buildings located inland was not changed significantly. However, the compound effect of 3.1 ft surge with a 24-h, 0.3 inch hr^{-1} storm event led to 46% increase in the number of inundated buildings to major flooding (~ 56,000 to ~ 82,000).

These results for the compounding of pluvial urban flooding with storm surge are based on a small number of scenarios and simulations with relatively conservative combinations of 90th percentile surge, as previously noted. While historical events with compounding have occurred (e.g., Irene), there have also been events with very little compounding (e.g., Ida, Sandy). To have a probabilistic understanding of the compounding of tide, surge and rain on NYC urban flooding, further analyses and a far larger simulation coverage of the multi-parameter space would be needed (Wahl et al. 2016; Bevacqua et al. 2019).

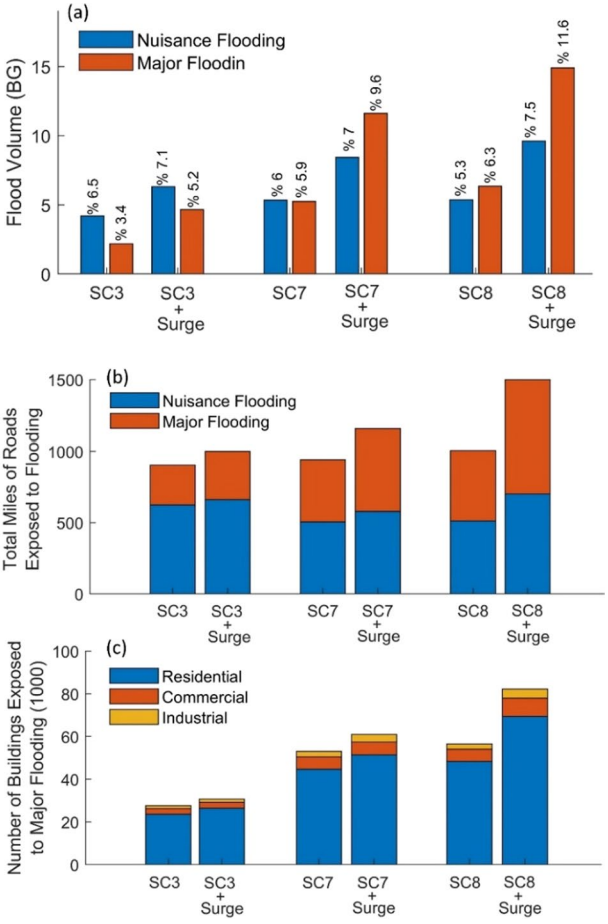

Fig. 8 The compounding effect of surge on **a** flood volume and extent **b** total miles of road exposed to nuisance and major flooding **c** number of buildings exposed to major flooding

3.4 Socioeconomic analysis

Figure 9 shows the number of exposed households/populations to flooding under different storm scenarios and sea-level conditions. In all storm scenarios, socioeconomically disadvantaged households (i.e., households with annual income less than $40,000), and underrepresented racial populations, were proportionally the most exposed group to flooding. The exposure of these vulnerable groups increased with higher sea-level conditions either due to SLR or surge.

While the 1-h, 1.77 inch hr^{-1} (SC3) and 24-h, 0.18 inch hr^{-1} (SC7) storm scenarios affected ~ 140,000 households with an annual income of less than $40,000, the more extreme 1-h storm scenario with average rainfall intensity of 3.66 inch hr^{-1} (SC4) affected ~ 240,000 households from the same group. The occurrence of the most extreme storm scenario by the time of the study (SC6) affected 365,000 households with an annual income of less than $40,000 and 1.5 million individuals from underrepresented racial populations. Considering 2.3 ft SLR by mid-century increased the number of low-income households from ~ 80,000 to ~ 110,000 and elevates the number of affected underrepresented populations by a factor of 1.3 (365,000 to 473,000). The compound effect of 3.1

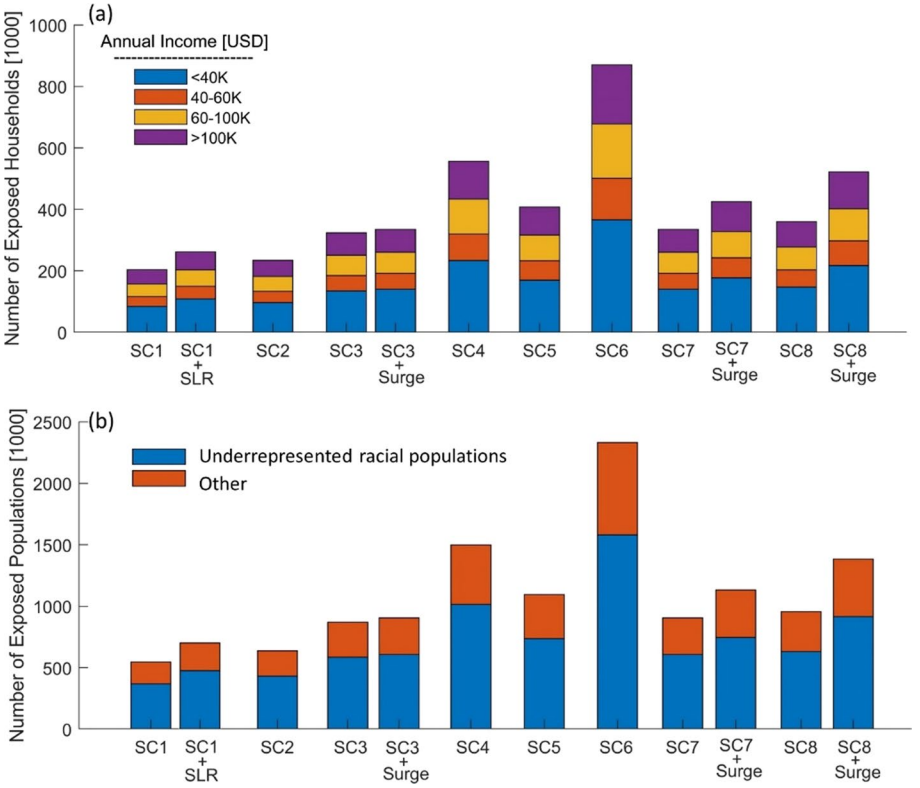

Fig. 9 The number of exposed people/households to flooding under different storm scenarios and sea-level conditions

ft surge with a 24-h, 0.3 inch hr^{-1} rainfall event led to a 48% increase in the number of exposed low-income households, and a 45% increase in the number of exposed people from ethnically diverse communities.

4 Discussion

This study represents a significant advancement in the NYC's efforts to enhance understanding of future storm events in the city and obtaining comprehensive understanding of flood hazards and exposure under these storm events and different sea-level conditions. The availability of past and current rainfall data in NYC is a valuable resource for understanding historical precipitation patterns. However, a critical gap in our knowledge emerges when considering future extreme rainfall events at sub-daily scales. While current datasets provide a robust foundation for understanding historical trends, predicting, and preparing for future extreme rainfall events required advancements in scientific research. Through this study we have addressed this gap that is essential for effective stormwater management and flood preparedness, especially in the context of climate change.

Twelve storm scenarios were thoughtfully designed in consultation with NYC stakeholders to meet specific city needs in emergency management, planning, and design.

They encompass a wide range of parameters, including current and future rainfall and tide scenarios as well as compound scenarios involving both rainfall and surge/SLR. The methodology employed to construct these scenarios involved advanced techniques such as extreme value analysis for assigning rainfall and surge depths, dynamic downscaling for rainfall time series, and the use of a coastal ocean model for offshore water-level time series. The creation and analysis of the storm scenarios offers a robust foundation for evaluating flood hazard and exposure in NYC.

The development of a set of H&H models for each sewershed across NYC represents a significant step in understanding the hazard and exposure related to different types of flooding, including pluvial and compound events involving storm surge. These models integrate 1-D stormwater components with 2-D overland flow simulations to provide a comprehensive analysis of flood scenarios. The creation of these models relied on various city data sources, including existing DEP sewer models, up-to-date DEMs, and land-use shapefiles. The model's resolution was based on a triangular mesh network, ensuring accurate representation with varying levels of detail. The validation of the citywide H&H model was a crucial step in ensuring its reliability and accuracy. This validation process involved model performance checks and a quantitative comparison of predicted flooding areas with historic flooding records, confirming the model's ability to simulate real-world conditions. Notable findings from these model simulations include the successful advancement of 1D and 2D stormwater modeling for NYC, encompassing a range of storm scenarios that account for SLR, storm surge, and variations in rainfall intensity.

The development and validation of H&H models for New York City's sewersheds represent a significant advancement in flood modeling and mitigation efforts. The ability to simulate a wide range of storm scenarios provides valuable insights for enhancing the city's resilience to flooding. However, ongoing refinement and improvements in stormwater modeling are necessary to fully harness the potential of these models for flood risk assessment and mitigation in the future. Specifically, in this study we did not account for the timing of rainfall. The omission of accounting for the timing of rainfall, particularly during peak hours, can significantly impact the assessment of flooding within a combined sewer system. Peak hours are characterized by heightened demand on sanitary sewers, creating a scenario where the system's capacity is already under stress. When rainfall coincides with these peak hours, the cumulative effect may lead to a more substantial strain on the system's ability to manage stormwater and sanitary flows. The interplay between stormwater runoff and the existing load on sanitary sewers during these high-demand periods can exacerbate flooding, potentially causing more pronounced and rapid inundation of urban areas.

The flood exposure analysis underscores the vulnerability of the stormwater system in NYC, particularly in the face of high-intensity short-duration "cloudburst" events. Our findings indicate a substantial impact, revealing that nearly one-third of NYC roads could potentially be inundated during such intense storm events. Notably, this stress on the stormwater system is further exacerbated under higher sea-level conditions, whether attributed to SLR or storm surge, resulting in an increased flood extent and volume. Socioeconomically disadvantaged households, characterized by an annual income of less than $40,000, and underrepresented racial populations are proportionally the most exposed groups to flooding. The exposure of these vulnerable groups is amplified under higher sea-level conditions. These insights contribute significantly to the study's overall goal of understanding the present and future exposure to urban pluvial flooding in NYC.

5 Conclusions

Here we developed a citywide H&H model to simulate flooding from stormwater in NYC and estimate citywide flood exposure under twelve storm scenarios. This is the first citywide analysis of rainfall-driven flooding using NYC's drainage models. Storm scenarios were defined such that they capture specific rainfall, surge, and SLR scenarios. The storm scenarios cover a wide range of rainfall intensity ranging from 0.3 to 4.3 inch hr^{-1}, with return periods from 1-year up to an approximately 10,000-year event, which was the worst historical rain event known to have occurred in the region by the time of this study. We demonstrated the potential for extensive flooding in NYC during intense, short-duration "cloudburst" events. Almost 18% of NYC could experience inundation during a 1-h, 3.6 inch hr^{-1} rainfall event. This value could rise to 28% in the case of a 3-h, 4.3 inch hr^{-1} storm event. We also investigated the impact of SLR and storm surge on stormwater propagation and found that increasing sea levels either from SLR and/or storm surge can lead to more extensive and severe flooding, as the NYC's gravity-drained sewer systems become less able to drain stormwater under higher sea-level conditions. We further showed that underrepresented and socioeconomically disadvantaged communities were proportionally the largest group exposed to flooding in NYC under all considered storm scenarios. These findings underscore the need for strategic planning and investment in the stormwater management system including gray infrastructure (i.e., centralized conveyance systems), green infrastructure (i.e., distributed infiltration systems), hybrid systems, and cloudburst management to reduce the risk of flooding and minimize potential damage to infrastructure and assets in the city.

Supplementary Information The online version contains supplementary material available at https://doi.org/10.1007/s11069-024-06466-8.

Acknowledgements This study was conducted in collaboration with the New York City Department of Environmental Protection and was partially supported by the National Science Foundation (NSF) Grant 1444758 as part of the Urban Water Innovation Network (UWIN) project. The statements made in this publication reflect solely the views of the individual authors and not the views of the funding agencies or affiliated institutions.

Funding This work was partially supported by the National Science Foundation (NSF) Grant 1444758 as part of the Urban Water Innovation Network (UWIN) project.

Data availability The hourly observed rainfall data are available from the NOAA's National Climatic Data Center (NCDC). (https://www.ncdc.noaa.gov/cdo-web/search). Building and land-use Information are available from MapPluto 2019 (https://www1.nyc.gov/site/planning/data-maps/open-data/dwn-pluto-mappluto.page).

Declarations

Conflict of interest The authors declare that they have no conflict of interest.

References

Atallah EH, Bosart LF (2003) The extratropical transition and precipitation distribution of hurricane Floyd (1999). Mon Weather Rev 131:1063–1081. https://doi.org/10.1175/1520-0493(2003)131%3c1063:TETAPD%3e2.0.CO;2

Avila LA, Cangialosi J (2011) Tropical cyclone report,Hurricane Irene

Bevacqua E, Maraun D, Vousdoukas MI et al (2019) Higher probability of compound flooding from precipitation and storm surge in Europe under anthropogenic climate change. Sci Adv 5:1–8. https://doi.org/10.1126/sciadv.aaw5531

Cappucci M (2019) Storms deluge New York City, abruptly ending sweltering heat wave. In: Washington Post. https://www.washingtonpost.com/weather/2019/07/23/flooding-rain-deluges-new-york-city-abruptly-ending-sweltering-heat-wave/?nid=top_pb_signin&arcId=GBWIDDMGIBEMJFKNSJ2HEZ73XM&account_location=ONSITE_HEADER_ARTICLE. Accessed 17 Jan 2023

Castellano CM, Degaetano AT (2017) Downscaled Projections of Extreme Rainfall in New York State Technical Document Cornell University Ithaca , NY. 1–25

Chen X, Zhang X, Church JA et al (2017) The increasing rate of global mean sea-level rise during 1993–2014. Nat Clim Chang 7:492–495. https://doi.org/10.1038/nclimate3325

Colle BA, Lombardo KA, Tongue JS et al (2012) Tornadoes in the New York metropolitan region: Climatology and multiscale analysis of two events. Weather Forecast 27:1326–1348. https://doi.org/10.1175/WAF-D-12-00006.1

Colle BA, Bowman MJ, Roberts KJ, et al (2015) Exploring Water Level Sensitivity for Metropolitan New York. J Mar Sci Eng 428–443. https://doi.org/10.3390/jmse3020428

Depietri Y, McPhearson T (2018) Changing urban risk: 140 years of climatic hazards in New York City. Clim Change 148:95–108. https://doi.org/10.1007/s10584-018-2194-2

Diakakis M, Deligiannakis G, Katsetsiadou K, Lekkas E (2015) Hurricane Sandy mortality in the Caribbean and continental North America. Disaster Prev Manag 24:132–148. https://doi.org/10.1108/DPM-05-2014-0082

Fieser E (2011) Hurricane Irene barrels toward US as Caribbean islands take stock of damage. In: Christ. Sci. Monit. Arch. https://www.csmonitor.com/World/Americas/2011/0825/Hurricane-Irene-barrels-toward-US-as-Caribbean-islands-take-stock-of-damage. Accessed 9 Mar 2022

Ganguli P, Paprotny D, Hasan M, et al (2020) Projected Changes in Compound Flood Hazard From Riverine and Coastal Floods in Northwestern Europe. Earth's Futur 8:. https://doi.org/10.1029/2020EF001752

Ghanbari M, Arabi M, Kao SC et al (2021) Climate Change and Changes in Compound Coastal-Riverine Flooding Hazard Along the U.S. Coasts Earth's Futur 9:1–17. https://doi.org/10.1029/2021EF002055

Ghanbari M, Arabi M, Obeysekera J, Sweet W (2019) A Coherent Statistical Model for Coastal Flood Frequency Analysis Under Nonstationary Sea Level Conditions Earth ' s Future. Earth 's Futur 7:162–177. https://doi.org/10.1029/2018EF001089

Gornitz V, Oppenheimer M, Kopp R, Orton P, Buchanan M, Lin N, Horton R, Bader D (2019) New York City panel on climate change 2019 report Chapter 3: sea level rise. In: Annals of the New York Academy of Sciences, vol 1439, no 1, pp 71–94. https://doi.org/10.1111/nyas.14006

Hallegatte S, Green C, Nicholls RJ, Corfee-Morlot J (2013) Future flood losses in major coastal cities. Nat Clim Chang 3:. https://doi.org/10.1038/NCLIMATE1979

Horton RE (1941) An Approach Toward a Physical Interpretation of Infiltration-Capacity. Soil Sci Soc Am J 5:399–417. https://doi.org/10.2136/sssaj1941.036159950005000c0075x

Horton R, Little C, Gornitz V et al (2015) New york city panel on climate change 2015 report chapter 2: Sea level rise and coastal storms. Ann N Y Acad Sci 1336:36–44. https://doi.org/10.1111/nyas.12593

Infoworks (2012) INFOWORKS: Citywide Recalibration Report

Jha AK, Bloch R, Lamond J (2012) A Guide to Integrated Urban Flood Risk Management for the 21st Century

Karamouz M, Zahmatkesh Z, Goharian E, Nazif S (2015) Combined impact of inland and coastal floods: Mapping knowledge base for development of planning strategies. J Water Resour Plan Manag 141:1–16. https://doi.org/10.1061/(ASCE)WR.1943-5452.0000497

Kemp AC, Hill TD, Vane CH et al (2017) Relative sea-level trends in New York City during the past 1500 years. Holocene 27:1169–1186. https://doi.org/10.1177/0959683616683263

Lenderink G, Van Meijgaard E (2010) Linking increases in hourly precipitation extremes to atmospheric temperature and moisture changes. Environ Res Lett 5:. https://doi.org/10.1088/1748-9326/5/2/025208

Li Z, Li C, Xu Z, Zhou X (2014) Frequency analysis of precipitation extremes in Heihe River basin based on generalized Pareto distribution. Stoch Environ Res Risk Assess 28:1709–1721. https://doi.org/10.1007/s00477-013-0828-5

Liu C, Ikeda K, Rasmussen R, Barlage M, Newman AJ, Prein AF, Chen F, Chen L, Clark, M, Dai A, Dudhia J, Eidhammer T, Gochis D, Gutmann E, Kurkute S, Li Y, Thompson G, Yates D (2017) Continental-scale convection-permitting modeling of the current and future climate of North America. Clim Dyn 49:71–95. https://doi.org/10.1007/s00382-016-3327-9

Lombardo KA, Colle BA (2010) The spatial and temporal distribution of organized convective structures over the Northeast and their ambient conditions. Mon Weather Rev 138:4456–4474. https://doi.org/10.1175/2010MWR3463.1

Moftakhari HR, Salvadori G, AghaKouchak A et al (2017) Compounding effects of sea level rise and fluvial flooding. Proc Natl Acad Sci 114:9785–9790. https://doi.org/10.1073/pnas.1620325114

NOAA (2014) National Oceanic and Atmo-spheric Administration (NOAA) Atlas 14 point precipitation frequency estimates. https://hdscnws.noaa.gov/hdsc/pfds/pfds_map_cont.html?bk-mrk=ny

NPCC (2015) NPCC 2015 Contributors and Reviewers. Ann N Y Acad Sci 1336:1–2. https://doi.org/10.1111/nyas.12626

NYC Stormwater Resiliency Plan (2021) NYC Stormwater Resiliency Plan

NYC DEP (2021) Sewer System. https://www1.nyc.gov/site/dep/water/sewer-system.page. Accessed 25 Jul 2022

NYDEC (2019) Climate Change Effects And Impacts - NYDEC. https://www.dec.ny.gov/environmental-protection/climate-change/effects-impacts

NYS (2018) NYS High Resolution DEM. https://gis.ny.gov/nys-dem. Accessed 30 Nov 2023

NYSDEC (2021) Observed and Projected Climate Change in New York State: An Overview AUGUST 2021. https://extapps.dec.ny.gov/docs/administration_pdf/ccnys2021.pdf

New York Times (2021) Heavy Rains Pound New York City, Flooding Subway Stations and Roads - The New York Times. https://www.nytimes.com/2021/07/08/nyregion/flooding-subways-nyc.html. Accessed 28 Jul 2022

Orton P, Georgas N, Blumberg A, Pullen J (2012) Detailed modeling of recent severe storm tides in estuaries of the New York City region. J Geophys Res 117:1–17. https://doi.org/10.1029/2012JC008220

Orton PM, Hall TM, Talke SA et al (2016) A validated tropical-extratropical flood hazard assessment for New York Harbor. J Geophys Res Ocean 121:8904–8929. https://doi.org/10.1038/175238c0

Pawlowicz R, Pawlowicz R, Beardsley RC et al (2002) Classical tidal harmonic analysis including error estimates. MATLAB Using T TIDE Comput Geosci 28:929–937

Rahmstorf S, Coumou D (2011) Increase of extreme events in a warming world. Proc Natl Acad Sci 108:17905–17909. https://doi.org/10.1073/pnas.1101766108

Rahmstorf S (2007) A Semi-Empirical Approach to Projecting Future Sea-Level Rise. Science (80-) 315:368–370

Rasmussen R, Liu C (2017) High resolution wrf simulations of the current and future climate of North America. Research data archive at the national center for atmospheric research, computational and information systems laboratory. https://doi.org/10.5065/D6V40SXP

Rossman L (2015) Storm Water Management ModelUser's Manual Version 5.1

Saleh F, Ramaswamy V, Wang Y et al (2017) A multi-scale ensemble-based framework for forecasting compound coastal-riverine flooding: The Hackensack-Passaic watershed and Newark Bay. Adv Water Resour 110:371–386. https://doi.org/10.1016/j.advwatres.2017.10.026

Sillmann J, Kharin VV, Zhang X et al (2013) Climate extremes indices in the CMIP5 multimodel ensemble: Part 1. Model evaluation in the present climate. J Geophys Res Atmos 118:1716–1733. https://doi.org/10.1002/jgrd.50203

Skamarock WC, Klemp JB (2008) A time-split nonhydrostatic atmospheric model for weather research and forecasting applications. J Comput Phys 227:3465–3485. https://doi.org/10.1016/j.jcp.2007.01.037

Smith B, Rodriguez S (2017) Spatial analysis of high-resolution radar rainfall and citizen-reported flash flood data in ultra-urban New York City. Water (Switzerland) 9:1–17. https://doi.org/10.3390/w9100736

Sweet WV, Kopp RE, Weaver CP, et al (2017) Global and Regional Sea Level Rise Scenarios for the United States. NOAA Tech Rep NOS CO-OPS 083

Wahl T, Jain S, Bender J et al (2015) Increasing risk of compound flooding from storm surge and rainfall for major US cities. Nat Clim Chang 5:1093–1097. https://doi.org/10.1038/nclimate2736

Wahl T, Plant NG, Long JW (2016) Probabilistic assessment of erosion and flooding risk in the northern Gulf of Mexico. J Geophys Res Ocean 121:3029–3043. https://doi.org/10.1002/2015JC011482

Walsh J, Wuebbles D, Hayhoe K et al (2014) Our Changing Climate. Clim Chang Impacts United States Third Natl Clim Assessment, J M Melillo, Terese Richmond, G W Yohe, Eds, US Glob Chang Res Progr. https://doi.org/10.7930/J0KW5CXT

Wolfe E, Schaeffer M, Sutton J, et al (2021) THE NEW NORMAL : COMBATING STORM-RELATED EXTREME WEATHER IN NEW YORK CITY

Yohe G, Leichenko R (2010) Chapter 2: Adopting a risk-based approach: Ch 2. Adopting a risk-based approach. Ann N Y Acad Sci 1196:29–40. https://doi.org/10.1111/j.1749-6632.2009.05310.x

Zscheischler J, Martius O, Westra S et al (2020) A typology of compound weather and climate events. Nat Rev Earth Environ 1:333–347. https://doi.org/10.1038/s43017-020-0060-z

Authors and Affiliations

Mahshid Ghanbari[1] · Tyler Dell[2] · Firas Saleh[3] · Ziyu Chen[4] · Jennifer Cherrier[5,6] · Brian Colle[7] · Joshua Hacker[8] · Luke Madaus[8] · Philip Orton[4] · Mazdak Arabi[1]

✉ Mahshid Ghanbari
mahshid.ghanbari@colostate.edu

[1] Department of Civil and Environmental Engineering, Colorado State University, Fort Collins, CO, USA

[2] City of Longmont, Longmont, CO, USA

[3] Moody's RMS, Newark, CA, USA

[4] Davidson Laboratory, Department of Civil, Environmental and Ocean Engineering, Stevens Institute of Technology, Hoboken, NJ, USA

[5] Department of Earth and Environmental Sciences, CUNY-Brooklyn College, Brooklyn, NY, USA

[6] CUNY-Graduate Center, Earth and Environmental Sciences, New York, NY, USA

[7] School of Marine and Atmospheric Sciences, Stony Brook University, Stony Brook, NY, USA

[8] Jupiter, Boulder, CO, USA